Signal, Image and Video Processing (2024) 18:7285–7291
https://doi.org/10.1007/s11760-024-03393-w

ORIGINAL PAPER

CFAR detection using two scale invariant functions in heterogeneous Weibull clutter

Khaled Zebiri[1] · **Amar Mezache**[2]

Received: 21 March 2024 / Revised: 18 May 2024 / Accepted: 19 June 2024 / Published online: 28 June 2024

Abstract

In this paper, we considered the constant false alarm rate (CFAR) detector in presence of Swerling 1 interfering targets surrounded in Weibull background. The proposed CFAR detector is inspired from a general test statistic that is given as a function of two selected scale invariant functions. It is based on the well known Weber-Haykin Order Statistics CFAR (WHOS-CFAR) detector and is given in terms of three ranked samples. Even in the face of several interfering targets, the investigation of the false alarm regulation demonstrates the robustness with respect to scale and shape clutter parameters. Moreover, through simulated and IPIX (Intelligent PIXel X-band radar) real data, the performance of the above WHOS-CFAR detector is checked for both homogeneous and heterogeneous environments and achieves the CFAR-ness property with immunity to circumstances involving interfering targets.

Keywords Weibull model · Interfering targets · WHOS-CFAR

1 Introduction

According to the change tendency in the sea clutter structural characteristics, target detection by high resolution maritime surveillance radar is somewhat complex [1, 2]. Usually, non-Gaussian distributions are applied to reveal statistical properties of this type of clutter parameters [3]. The Weibull clutter model is of significant interest to many academics studying radar signal processing since it fits a wide range of clutter types under different conditions when it comes to X-band high resolution maritime surveillance radar clutter target detection [4, 5]. For X-band maritime models with low grazing angle and different range resolutions, it successfully characterizes the heavy tails of sea clutter because its parameters and Probability Density Function (PDF) are easily estimated [6–8]. The creation of CFAR techniques is quite complex in this setting, especially when researchers are attempting to detect with unknown clutter characteristics [9, 10] in heterogeneous environments. Many non-coherent CFAR detectors with unknown parameters have been built for the case of Weibull, log-normal, and Pareto clutter models [6, 11, 12]. For example, in the presence of Weibull and log-normal disturbances, various CFAR detectors are proposed, such as logt-CFAR, Maximum Likelihood (ML) CFAR, [zlog(z)]-CFAR, Trimmed Mean Order Statistic (TMOS) CFAR, and Robust Variability Index (RVI) CFAR [12]. Weinberg et al. [13] have proposed the use of Bayesian-CFAR and Geometric Mean (GM) CFAR techniques for Pareto type II and Pareto type I clutter models. Fully CFAR properties are maintained for any values of scale and shape parameters. CFAR detector in the presence of numerous targets embedded in log-normal and Pareto type I clutter have been proposed recently by Zebiri and Mezache [4]. Here, a general decision process provided in [5] is used to create four-order statistics-based CFAR detector. If other distributions like gamma, K, generalized-K and KK are considered for sea echoes, non-coherent CFAR detection problems with uncertain scale and shape parameters have yet to be solved due to the mathematical difficulties of integral computations [13].

Motivated by the previous CFAR detectors in heterogeneous Weibull background, in this paper, a novel WHOS-CFAR detector is proposed to accomplish the combination

✉ Khaled Zebiri
k.zebiri@univ-alger.dz

Amar Mezache
amar.mezache@univ-msila.dz

1 Département des Sciences de la matière (SM), Université d’Alger « 1 » Benyoucef benkhadda, Alger centre 16000, Algeria

2 Département d’électronique, Université Mohamed Boudiaf M’sila, M’sila 28000, Algeria

of OS-CFAR and WH-CFAR algorithms based on the selection of two invariant non-negative functions. In the proposed detector, the threshold is derived in terms of three-order statistics maintaining a full CFAR property for unknown Weibull clutter parameters. From multiple tests, the ranks of the sorted samples are selected from the simulated data, offering a trustworthy assessment of the clutter level. Simulation findings demonstrate the appropriateness of the proposed detector in the presence of strong interfering targets. The authors in [5] discuss the theoretical foundations of such CFAR detection. In order to produce a dependable CFAR detector in the face of numerous interfering targets, our effort concentrated on utilizing the optimal combination of functions h and g. As such, the work only makes passing reference to theoretical material.

The paper is organized as follows. The Weibull model is introduced in Sect. 2 along with the suggested WHOS-CFAR detector derived from a general scale invariant test statistic of the clutter model with unknown parameters. Section 3 uses synthetic Weibull distributed samples for comparison purposes between the aforesaid CFAR algorithms in terms of CFAR characteristics and detection probability. Section 4 verifies the robustness of the suggested detector using IPIX real data. Section 5 provides a summary of the primary findings of this study.

2 CFAR algorithm using Weber–Haykin and order statistics

It has been discovered that the Weibull distribution accurately describes radar backscattering from both land and sea. The Weibull distribution with a scale parameter $b > 0$ and a shape parameter $c > 0$, X, has the PDF defined by [7].

$$p(x) = \frac{c}{b}\left(\frac{X}{b}\right)^{c-1} \exp\left(-\left(\frac{X}{b}\right)^{c}\right), \quad x > 0 \tag{1}$$

Clutter models have frequently been based on log-normal and Weibull variates in radar CFAR detection problems. The test statistics shown here are a summary of the detectors used in homogeneous and heterogeneous Weibull and log-normal clutter, namely the logt-, WH-, GMOS-, TMOS-, TS- and IE-CFAR detectors. The class of random variables that includes the random variable X specified by (1) is called scale and power invariant distributions. Given by is the general decision rule.

$$\mathrm{T}(\mathrm{X}_0, \mathrm{X}_1, \ldots, \mathrm{X}_\mathrm{N}) \underset{H_0}{\overset{H_1}{\gtrless}} \tau \tag{2}$$

In which the Cell Under Test (CUT) is denoted by X_0 and the Clutter Range Profile (CRP) by $(X_1, X_2, \ldots, X_N)$, and the test statistic of the aforementioned CFAR algorithms is given as $T(X_0, X_1, \ldots)$. Where N is the sample size and is the scaling factor, which is dependent on the intended value of the false alarm probability (P_{FA}). With a test statistic provided by [7], Goldstein suggested an automatic logt-CFAR detector in both log-normal and Weibull clutter that preserves a CFAR property when there are no outliers (homogeneous clutter case).

$$\log(X_0) \underset{H_0}{\overset{H_1}{\gtrless}} \hat{\mu} + \hat{\sigma}\tau \tag{3}$$

where, respectively, $\hat{\mu}$ and $\hat{\sigma}$ represent the $log(X)$ mean and standard deviation. Interfering targets inside the CRP can significantly reduce the performance of the CFAR detector. To mitigate this degradation, Weber and Haykin constructed the test statistic as a function of the dual order statistics supplied by (4) [14].

$$X_0 \underset{H_0}{\overset{H_1}{\gtrless}} X_{(i)}^{1-\tau} X_{(j)}^{\tau} \tag{4}$$

With the proviso that $i \neq j$, so that (4) is meaningful.

The primary discovery in [5] is that, if the underlying clutter model is part of a class of scale and power invariant, then the adaptive detection threshold T can show the following general hypothesis test

$$X_0 \underset{H_0}{\overset{H_1}{\gtrless}} \underbrace{g(X_1, X_2, \ldots, X_N) e^{\tau h\left(\log\left(\frac{x_1}{g(X_1, X_2, \ldots, X_N)}\right), \ldots, \log\left(\frac{x_N}{g(X_1, X_2, \ldots, X_N)}\right)\right)}}_{T} \tag{5}$$

where τ is the scale factor used to modify the intended P_{FA}, X_0 is the CUT, $X_1, X_2, \ldots, X_N$ are iid (independent and identically distributed) clutter samples, $h(.)$ and $g(.)$ are two scale-invariant non-negative functions calculated from the CRP. According to hypothesis H_1, if X_0 exceeds T, the target is announced. The contrary hypothesis, H_0, suggests that the target is nonexistent when X_0 is smaller than T.

To ensure the CFAR property, $g(.)$ and $h(.)$ must be chosen appropriately. seven CFAR detectors for Weibull radar clutter have been proposed in the open literature with the labels WH-, GMOS-, TMOS-, IE-, TS- and TMOS-CFAR detectors [5]. These detectors are based on (5). In this work, several trials and errors are conducted for the case of Weibull clutter in order to determine underlying scale invariant functions to be

$$\begin{cases} g(X_1, X_2, \ldots, X_N) = X_{(i)}^{1-\tau} X_{(j)}^{\tau} \\ h(X_1, X_2, \ldots, X_N) = X_{(K)} \end{cases} \tag{6}$$

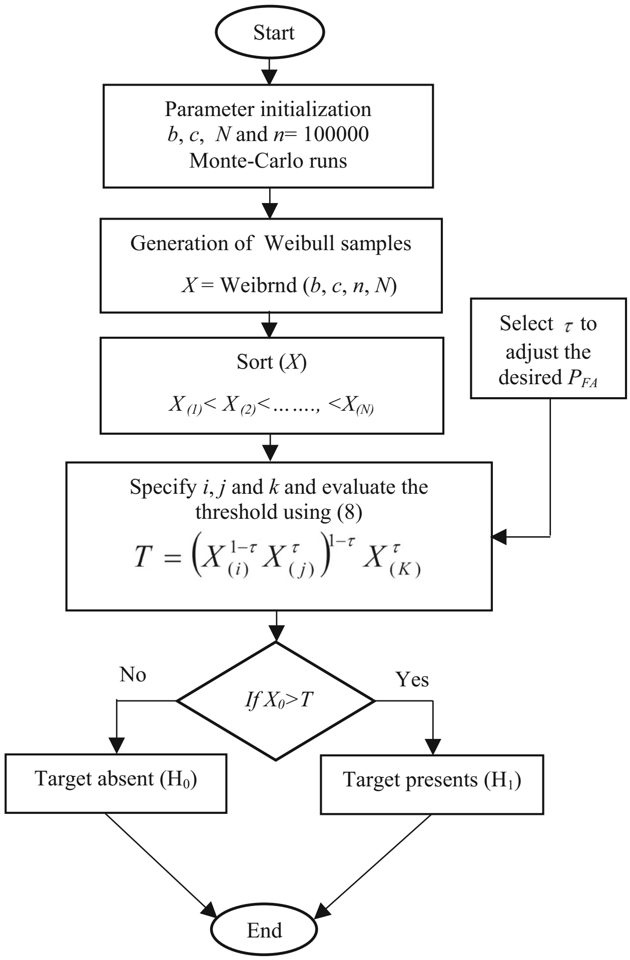

Fig. 1 Flow-chart of WHOS-CFAR algorithm in Weibull clutter

Substituting (6) into (5), the adaptive threshold in (5) becomes

$$T = \left(X_{(i)}^{1-\tau} X_{(j)}^{\tau}\right) e^{\tau h\left(\log\left(\left(\frac{x_1}{X_{(i)}^{1-\tau} X_{(j)}^{\tau}}\right), \ldots\ldots, \log\left(\frac{x_N}{X_{(i)}^{1-\tau} X_{(j)}^{\tau}}\right)\right)\right)} \tag{7}$$

Simplifying (7), the novel threshold of WHOS-CFAR detector is obtained

$$T = \left(X_{(i)}^{1-\tau} X_{(j)}^{\tau}\right)^{1-\tau} X_{(K)}^{\tau} \tag{8}$$

$$X_0 \underset{H_0}{\overset{H_1}{\gtrless}} \left(X_{(i)}^{1-\tau} X_{(j)}^{\tau}\right)^{1-\tau} X_{(K)}^{\tau} \tag{9}$$

A flowchart is shown in Fig. 1 to demonstrate how the WHOS-CFAR algorithm for target detection in Weibull clutter operates.

We then resort to the method of choosing these two non-negative functions *g(.)* and *h(.)* to generate a new decision rule that is immune to the existence of strong interfering targets (the capture effect). In order to do this, in the presence of Weibull clutter disturbances, the WHOS-CFAR detection technique, based on triple order statistics, is proposed. This study aims to explain the idea of selecting two functions, *h* and *g*, to create a special threshold that can handle interferences (a mix of WH and OS).

The established CFAR algorithms listed above were obtained by applying certain mathematical operations following the explanation of *g(.)* and *h(.)*. The purpose of the next section is to use (8) to illustrate the CFAR property and improved detection probability.

In the following part, we will look at how the suggested CFAR algorithm (8) behaves for Weibull clutter embedded Rayleigh targets in environments with either a homogeneous or heterogeneous Weibull domain.

3 Detection assessments

The detection performance for a finite length of the CRP N when Weibull clutter surrounds Rayleigh targets is investigated using Monte-Carlo simulations. The relationship between P_{FA} and clutter parameters is investigated for the innovative CFAR algorithm. In all simulations, N is set to 32 and P_{FA} is fixed at 10^{-3} to guarantee that at least 100,000 trials are required for the best threshold estimation. To make it possible to evaluate detection losses. It comes with the ideal detector. Where $X_0 \underset{H_0}{\overset{H_1}{\gtrless}} b(-\log(P_{FA}))^{\frac{1}{c}}$ is the optimal threshold that remains unaffected by the clutter's heterogeneity We shall compare the WHOS-CFAR's performance to that of the logt-, GMOS-, TMOS-, IE-, and WH-CFAR detectors.

3.1 Evaluation of performance in homogeneous domain

The P_{FA} is outlined of homogeneous and heterogeneous Weibull clutter conditions for a range of values of b. Following several tests, the optimal choice of the three ordering parameters of WHOS-CFAR was determined to be ($i = 1, j = 10, k = 27$). In Fig. 2b, we plot the detection performance of the WHOS-CFAR detector comparing with (GMOS, TMOS, and IE)–CFARs detectors, including the log-t detector in homogeneous Weibull clutter. As can be seen in the curve of Fig. 2b, the log-t provides the highest detection for homogeneous environment comparing with the other detectors. These observations, along with the fact that the curves almost overlap regardless of the value of b, demonstrate that the proposed threshold is CFAR for this type of clutter to an acceptable extent.

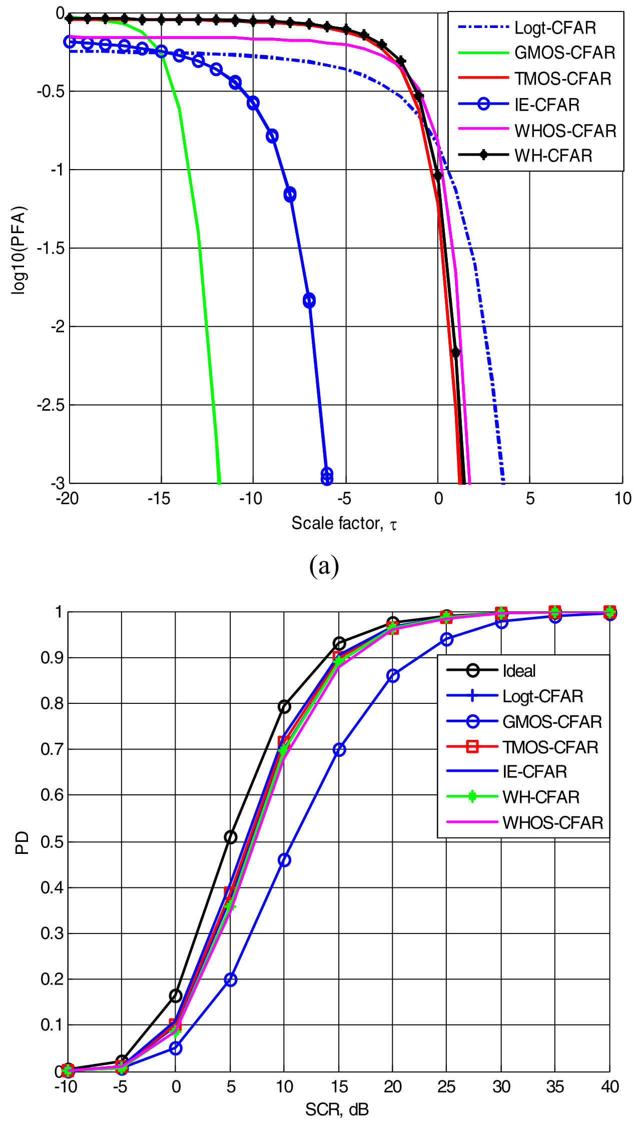

Fig. 2 Performance of WHOS-CFAR algorithm for homogeneous Weibull clutter, $N = 32$ and $P_{FA} = 10^{-3}$. **a** CFAR property against τ with $b = 0.1, 0.5, 1$ and 2, **b** P_D values against SCR with $b = 1$ and $c = 1$

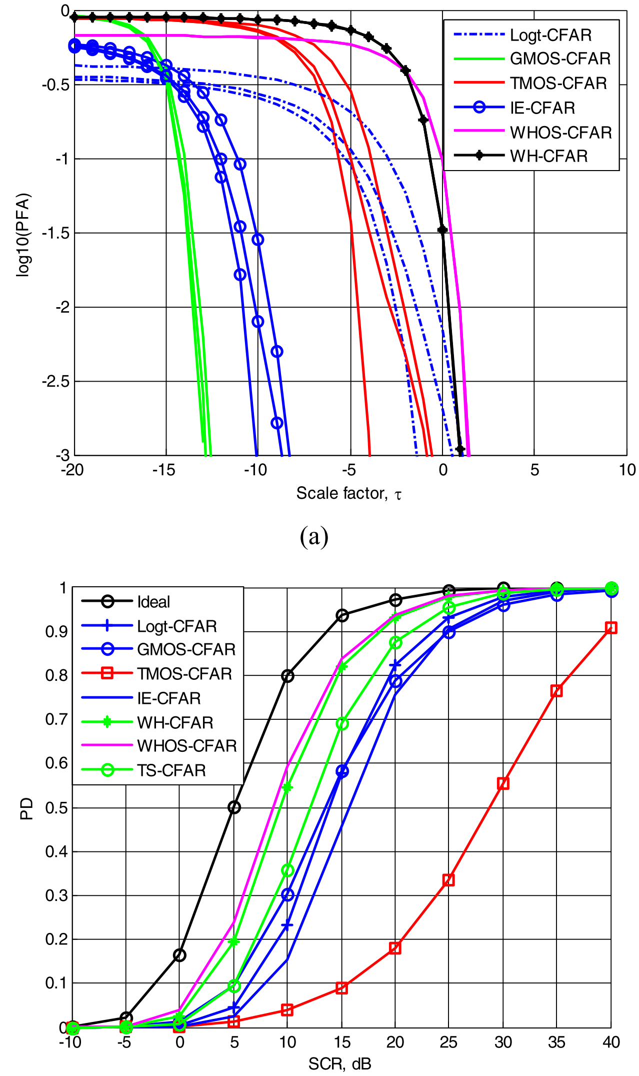

Fig. 3 Performance of WHOS-CFAR algorithm for heterogeneous Weibull clutter with 2 interfering targets injected at 8th and 24th range cells, $N = 32$. **a** CFAR property against $c = 0.1, 0.5, 1$ and 2, **b** P_D values against SCR with $b = 1$ and $c = 1$

3.2 Evaluation of performance in non-homogeneous domain (interfering targets)

This section evaluates the suggested triple order statistics (WHOS-CFAR) against interfering targets for Weibull clutter. We assess false alarm regulation performance in the presence of interfering targets by inserting two, three, and four strong targets in reference cells with an Interference to Clutter Ratio (ICR) of 20 dB.

Figures 2, 3 and 4 show the injection of two, three, and four interfering targets into the reference window, respectively. The novel WHOS-CFAR algorithm improves immunity, and consequently the CFAR loss decreases as shown in Figs. 2a, 3a, 4a and 4b. The P_{FA} is maintained even for a very spiky clutter and consequently the suggested detector retains its robustness, demonstrating that the proposed detection threshold is CFAR for Weibull model. Note that, the divergence of the P_{FA} is directly proportional to the number of targets. This is due to decreased estimation accuracy of clutter level from the CRP in the CUT.

The results of P_D values versus SCR for $c = 1$ and $b = 1.5$ in Weibull clutter are presented in Figs. 2b, 3b and 4c. In these curves, as can be observed, the proposed detector gives the best performance in the presence of multiple interfering targets and exhibits low detection losses compared to existing

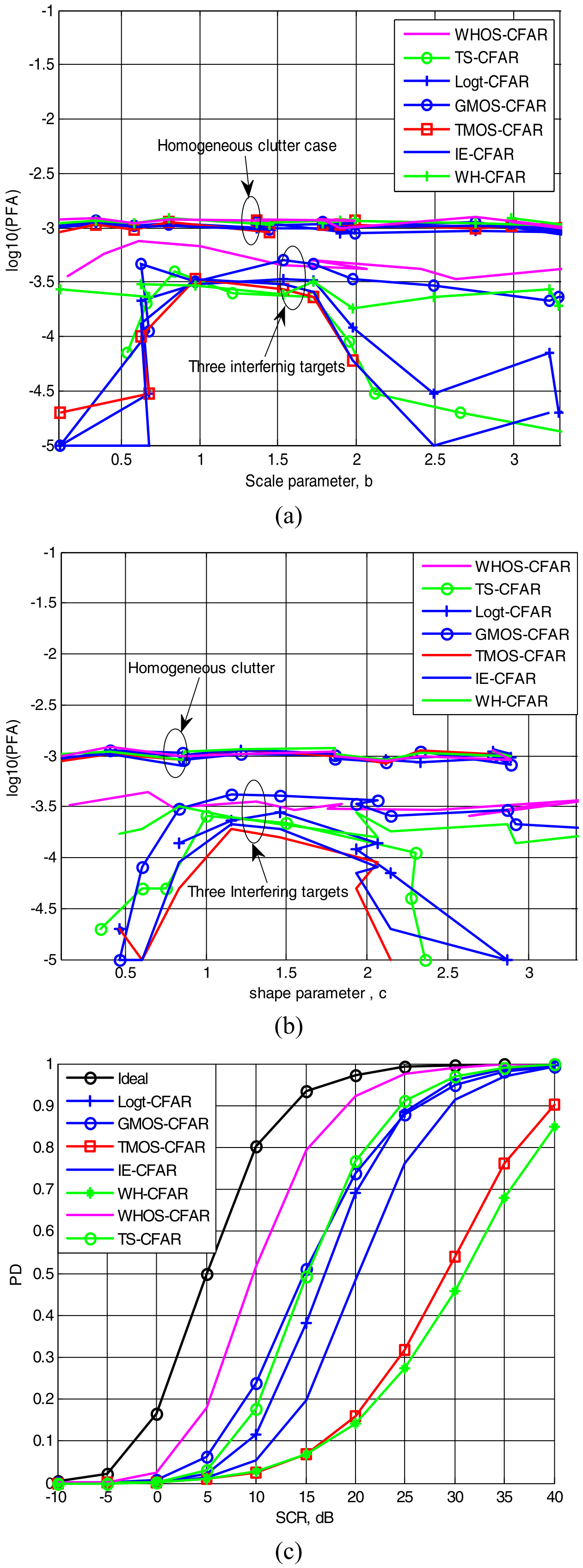

Fig. 4 Performance of WHOS-CFAR algorithms for heterogeneous Weibull clutter with 3 interfering targets injected at 7th, 13rd and 28th range cells, $N = 32$, ICR = 20db. **a** CFAR property against $b = 0.1$, 0.5, 1 and 2, **b** CFAR property against $c = 0.1$, 0.5, 1 and 3, **c** P_D values against SCR with $b = 1.5$ and $c = 1$

CFAR procedures. When the number of strong secondary targets increases, performances degradation of all CFAR algorithms were observed, but the WHOS-CFAR detector provides always the best CFAR loss. Note that, analytical expressions of the P_{FA} cannot be obtained for existing and proposed CFAR detectors. The CFAR property is demonstrated numerically under the condition of a class of scale invariant distribution of the clutter.

Note that, the performance of WH is directly landing, he can't resist due to the number of strong targets injected in the reference window. Here lies the role of our proposed detector who provides more immunity and resistance against strong multiple interfering targets, from simulated data, the highest curve corresponding to the WHOS-CFAR detector indicating that its CFAR loss is always smaller than the CFAR losses of the other CFAR algorithms.

In [15], a two parameter CFAR detector based on Truncated Clutter Statistics (TS-CFAR) detector was built using the truncated Weibull clutter statistics through the maximum likelihood estimators. We examined the TS-CFAR detector against non-homogeneous Weibull clutter. Figures 3b, 4b and 5b illustrate detection probability evaluation of the different CFAR algorithms. From the curves in Figs. 3a, 4a and 5a, A slight superiority of the WHOS-CFAR detector against the TS-CFAR algorithm is observed. In general, the WHOS-CFAR detector guaranties best detection performances, while keeping smallest P_{FA} deviations with respect to a desired P_{FA} $= 10^{-3}$.

4 Performance assessment using real data

The actual McMaster IPIX radar totally polarimetric measurement data is used to examine the P_{FA}'s regulation and validate the resilience of the suggested detectors. In 1984, the experimental instrumentation class radar known as the IPIX radar was launched. With 60,000 sweeps per cell, it is a polarimetric, coherent X-band radar [16, 17]. The three range resolutions—3 m, 15 m, and 30 m—as well as the horizontal and vertical polarizations were included in the study. The variation of P_{FA} as a function of τ is displayed in Fig. 6a. At the tenth range cell, we injected one interfering target injected at the 10th range cell with an ICR of 20 dB. The curve simulates the relationship between the WHOS-CFAR detector and the P_{FA}. After a great deal of trial and error, the optimal ordering matching the WHOS-CFAR algorithms were found to be $(i = 1, j = 30, k = 5)$. The P_{FA} curve nearly overlaps, indicating that the suggested algorithm preserves roughly the same P_{FA} value, with the exception of minor P_{FA} values where additional samples are required for improved accuracy. In Fig. 6b, P_D values are plotted as a function of SCR. Approximations of the WHOS-CFAR performance in comparison to results from IE-CFAR, TMOS, WHOS, and

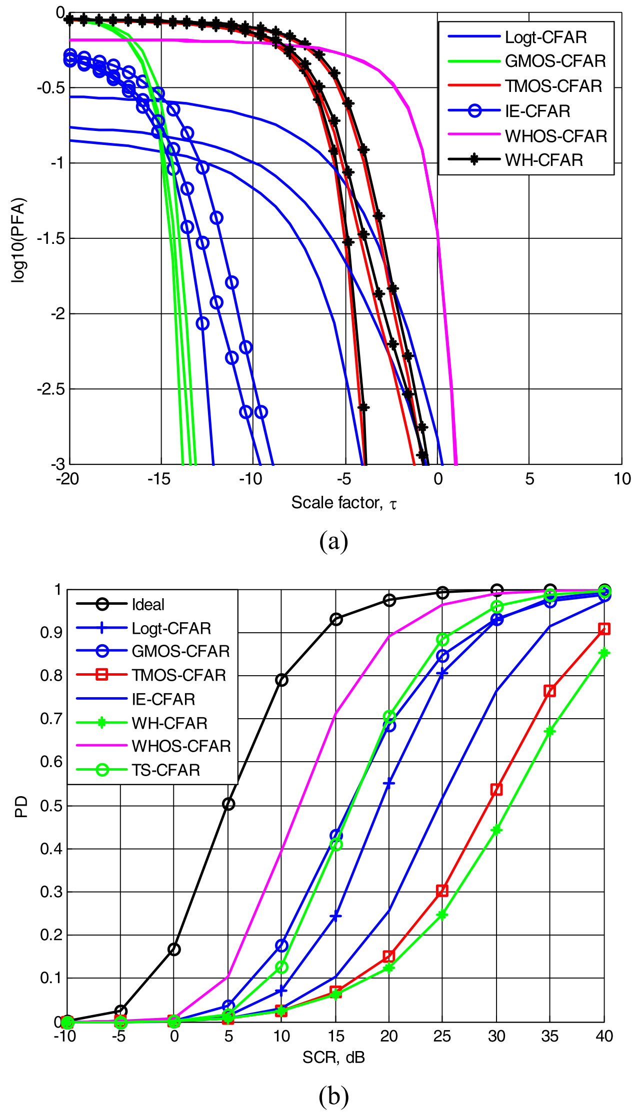

Fig. 5 Performance of logt-, GMOS-, TMOS-, IE-, WH-, TS- and WHOS-CFAR detectors for heterogeneous Weibull clutter with 4 interfering targets injected at 8th, 5th, 25th and 30th range cells, $N = 32$ and ICR = 20dB. **a** P_{FA} against the scale factor τ with $c = 0.1$, 0.5, 1 and 2, **b** P_D versus SCR with $b = 2$ and $c = 1$, **b** P_D values against SCR with $b = 1.5$ and $c = 1$

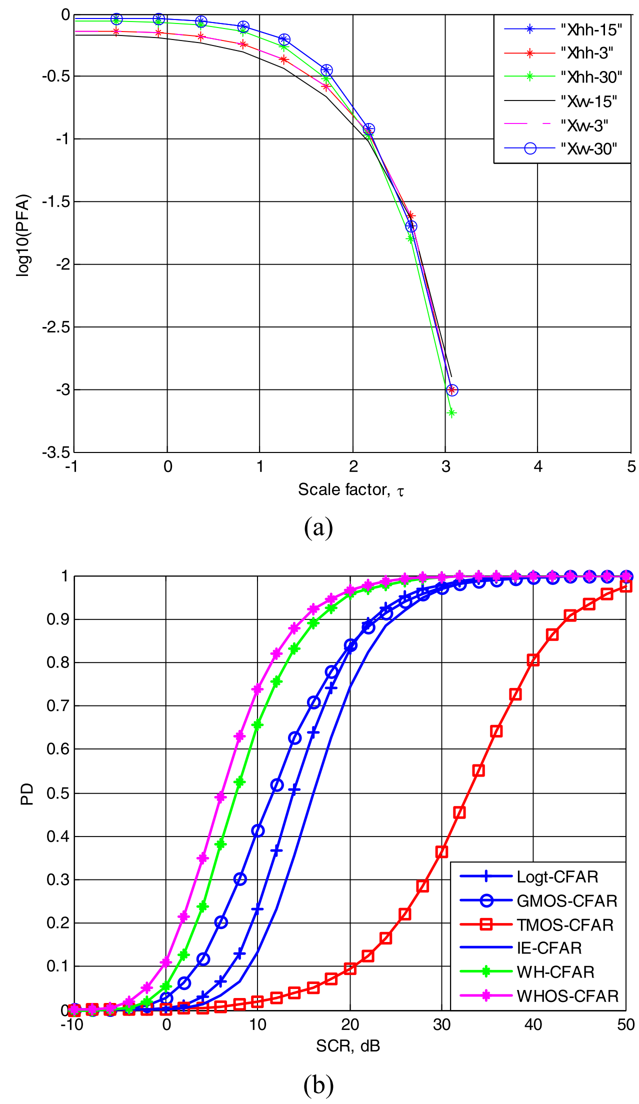

Fig. 6 Performance of the WHOS—CFAR detector using IPIX real Data. **a** Heterogeneous clutter caused by one interfering target injected at the 10th range cell. **b** *PD* versus SCR with resolution "Xvv-3" of *IPIX* real data with one interfering target with ICR = 20 dB injected at the 10th range cell

GMOS-CFAR provide the best detection performance for a given SCR.

5 Conclusion

Two scale invariant functions based CFAR detection in heterogeneous Weibull environment with unknown parameters was obtained firstly. To accomplish this, a general test statistic was considered and two non-negatives scale invariant functions were selected based on OS and WH statistics. The CFAR property was confirmed in terms of the scale and the shape parameters of the clutter model. The suggested receiver's detection probability is illustrated alongside that of existing techniques, with the proposed one showing its advantage in the scenario of numerous strong interfering targets.

Author contributions zebiri khaled: contribution+wrote the main manuscript text and prepared figures Amar Mezache; (correction of manuscript text)

Funding The authors declare that this paper was not funded by any institution.

Data availability The authors declare that there is no datasets or materials used in this paper.

Declarations

Conflict of interest The authors declare the following financial interests/personal relationships which may be considered as potential competing interests.

References

1. Barton, D.K.: Radar Clutter. Artech House Third printing, Washington, USA (1983)
2. Liu, W., Liu, J., Hao, C., Gao, Y., Liang Wang, Y.: Multichannel adaptive signal detection Basic theory and literature review. SCIENCE CHINA Inf. Sci. **65**(2), 121–301 (2022)
3. Anastassopoulos, V., Lampropoulos, G., Drosopoulos, A., Rey, N.: High resolution radar clutter statistics. IEEE Trans. Aerosp. Electron. Syst. **35**(1), 43–60 (1999)
4. Zebiri, K., Mezache, A.: Radar CFAR detection for multiple-targets situations for Weibull and log-normal distributed clutter. SIViP **15**, 1671–1678 (2021)
5. Weinberg, G.V., Bateman, L., Hayden, P.: Development of non-coherent CFAR detction processes in Weibull background. Digital Signal Process. **75**, 96–106 (2018)
6. Goldstein, G.B.: False-alarm regulation in Weibull and log-normal clutter. IEEE Trans. Aerosp. Electron. Syst. **AES-9**(1), 84–92 (1973)
7. Barkat, M.: Signal Detection and Estimation, 2nd edn. Artech House, Norwood, MA (2005)
8. Bentoumi, A., Mezache, A. Performance of non-parametric CFAR detectors in log-normal and *K* radar clutter. *3rd International Conference on Electrical Sciences and Technologies in Maghreb (CISTEM)*, 28–31October, Algiers, Algeria (2018).
9. Gouri, A., Mezache, A., Oudira, H.: Radar CFAR detection in Weibull clutter based on zlog(z) estimator. Taylor & Francis, Rem. Sens. Lett. **11**(6), 581–589 (2020)
10. Schleher, D.C.: Radar detection in Weibull clutter. IEEE Trans. Aerosp. Electron. Syst. **AES-12**(6), 736–743 (1976)
11. Wang, X., Li, Y., Zhang, N.: A robust variability index CFAR detector for weibull background. IEEE Trans. Aerosp. Electron. Syst. **59**(2), 2053–2064 (2022)
12. Weinberg, G.V., Alexopoulos, A.: Analysis of a dual order statistic constant false alarm rate detector. IEEE Trans. Aerosp. Electron. Syst. **52**(5), 2567–2574 (2016)
13. Weinberg, G.V., Howard, S., Tran, C.: Bayesian framework for detector development in pareto distributed clutter. IET Radar Sonar Navig. **13**(9), 1548–1555 (2019)
14. Weber, P., Haykin, S.: Ordered statistic CFAR processing for two-parameter distributions with variable skewness. IEEE Trans. Aerospace Electron. Syst. **AES-21**(6), 819–821 (1985)
15. Jiaqiu, A., Xuezhi, Y., Song, J., Dong, Z., Jia, L., Zhou, F.: An adaptively-truncated clutter-statistics-based two parameter CFAR detector in SAR imagery. IEEE J. Ocean. Eng. **43**(1), 267–279 (2018)
16. Bakker, R., Currie, B. The McMaster IPIX radar sea clutter database. (2020)
17. Zebiri, K., Mezache, A.: Quadruple-order statistics CFAR algorithm for Pareto type I environment. SIViP **18**(2), 1–7 (2023)